WHAT IS A "MASSIVE" CONCRETE STRUCTURE AT EARLY AGES? SOME DIMENSIONAL ARGUMENTS

By Franz-Josef Ulm,[1] Member, ASCE, and Olivier Coussy[2]

ABSTRACT: The risk of early-age concrete cracking depends on the capacity of hardening concrete to support the thermal stresses caused by the exothermic nature of the hydration process. This has been recognized for "massive" concrete structures. However, with the increasing use of high performance concretes, it is apparent that this problem also concerns traditionally "thin" structural members (columns, beams). The definition of a "massive" concrete structure, and how the structural dimension affects intensity and occurrence of chemically-induced strucctural degradation is the main focus of this paper. Based on dimensional analysis of the governing equations, a characteristic length scale, the hydration heat diffusion length, is derived; beyond this length the structure needs to be considered as "massive," and latent hydration heat effects affect the long-term structural integrity. From experimental data of normal strength concrete and high performance concrete, it is shown that this hydration heat diffusion length of high performance concrete is of the order of $\ell_h = 0.2$ m, and $l_h = 0.3$ m for normal strength concrete. Through a number of case studies, the relevant similarity parameters of the risk of early-age concrete cracking are identified, which allow's the monitoring of the structural performance of early-age concrete structures.

INTRODUCTION

It is well-known that the exothermic nature of the hydration reaction leads to temperature rises in "massive" concrete structures that induces a high risk of early-age concrete cracking during cooling and of premature structural degradation. This is a result of the combined effects of heat diffusion

$$C\,\frac{\partial\theta}{\partial t} = Q^\circ + l\,\frac{d\xi}{dt} \tag{1}$$

and hydration kinetics

$$\frac{d\xi}{dt} = \bar{A}(\xi)\exp\left(-\frac{E_a}{R\theta}\right) \tag{2}$$

In (1) and (2), the (absolute) temperature θ and the hydration degree $\xi \in [0; 1]$ are the unknown. The hydration degree is defined (Powers and Brownyard 1948) as the water mass m_{sk} normalized by the mass $m_{sk}(\infty)$ required for a complete hydration of the cement in the concrete mix:

$$\xi(t) = \frac{m_{sk}(t)}{m_{sk}(\infty)}; \quad 0 \le \xi \le 1 \tag{3}$$

From the stoichiometry of the hydration reactions, $m_{sk}(\infty) = 0.2c$, with c the amount of cement in the mix. Furthermore, C, l, E_a/R represent the volume heat capacity, the latent hydration heat, and the thermal activation constant (typically $E_a/R = 4000$ K); Q° is the rate of external heat supply, by conduction and volume heat sources (cooling pipes in early-age concrete structures); and $\tilde{A}(\xi)$ is the normalized hydration affinity (Ulm and Coussy 1996; Hellmich et al., 1999; Cervera et al. 1999), an intrinsic material function for concrete. It is independent of particular field and related boundary conditions. There are several ways to determine this kinetics function, but the easiest is by a calorimetric test. For instance, if we consider adiabatic conditions, it is $Q^\circ = 0$ in (1), and the heat equation integrates to

$$\xi(t) = \frac{1}{L}\,[\theta^{ad}(t) - \theta_0] \leftrightarrow L = l/C = \theta_\infty^{ad} - \theta_0 \tag{4}$$

where $\theta^{ad}(t)$ is the adiabatic temperature rise, and θ_0 and θ_∞^{ad} denote the initial and asymptotic temperature in the considered experiment. Using (4) in (2) determines the normalized affinity, as a function of time t in the adiabatic experiment

$$\tilde{A}(t) = \frac{1}{L}\,\frac{d}{dt}\,[\theta^{ad}(t) - \theta_0]\exp\left(\frac{E_a}{R\theta^{ad}(t)}\right) \tag{5}$$

By replacing time t in (5) by hydration degree ξ according to (4), the sought kinetics function $\tilde{A}(\xi)$ is obtained. Fig 1 shows the adiabatic temperature rise for a normal strength concrete ($f_c = 25$ MPa, $w/c = 0.6$) and a high performance concrete ($f_c = 80$ MPa, $w/c = 0.4$, $s/c = 0.1$). The corresponding normalized affinity $\tilde{A}(\xi)$ determined from (4) and (5) is given in Fig. 2.

The adiabatic case $Q^\circ = 0$ can be considered an asymptotic case of an infinite "massive" structure. On the contrary, isothermal conditions correspond to the other asymptote of an infinite "thin" structure, in which the heat generated by hydration is directly evacuated to maintain constant temperature, $\theta = \theta_0$. Real-life structures are in between. What is a "mas-

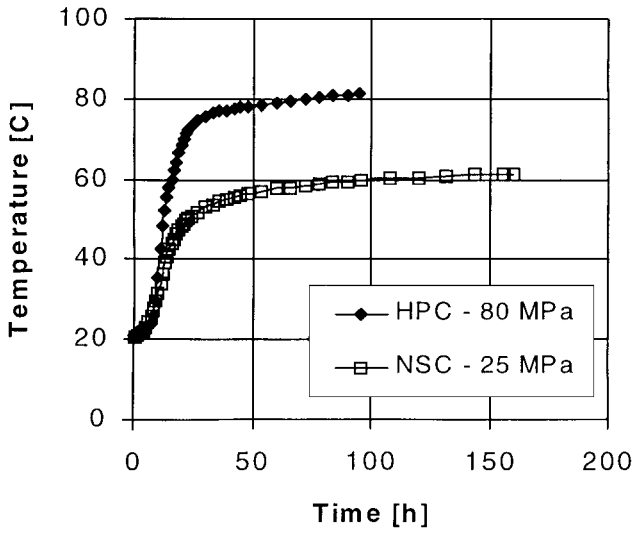

FIG. 1. Adiabatic Temperature Curve for High Performance Concrete (HPC) and Normal Strength Concrete (NSC)

[1]Assoc. Prof., Engrg. and Envir. Mech., Massachusetts Inst. of Technology, Cambridge MA 02139. E-mail: ulm@MIT.EDU

[2]Res. Dir., Laboratoire Central des Ponts et Chaussées, Department for Engineering Models, 58 Bd. Lefebvre, 75732 Paris Cedex 15, France.

Note. Associate Editor: Arup Maji. Discussion open until October 1, 2001. To extend the closing date one month, a written request must be filed with the ASCE Manager of Journals. The manuscript for this paper was submitted for review and possible publication on March 29, 2000; revised December 19, 2000. This paper is part of the ***Journal of Engineering Mechanics***, Vol. 127, No. 5, May 2001. ©ASCE, ISSN 0733-9399/01/0005-0512–0522/$8.00 + $.50 per page. Paper No. 22281.

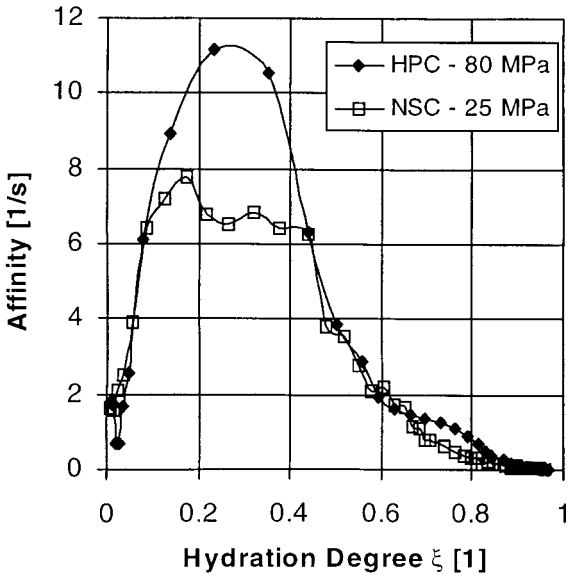

FIG. 2. Normalized Affinity for High Performance Concrete (HPC) and Normal Strength Concrete (NSC)

sive'' structure, and how does this structural dimension affect intensity and occurrence of chemically induced structural degradation is a key question considered in this paper.

CHARACTERISTIC HYDRATION HEAT DIFFUSION LENGTH

A characteristic length scale, beyond or below which the structure can be considered as ''massive'' or ''thin'' needs to be derived importance.

For this purpose, we consider the semiinfinite half-space $x > 0$, the idealized 1D-heat diffusion equation

$$\frac{\partial(\theta - \theta_0)}{\partial t} = D\,\frac{\partial^2(\theta - \theta_0)}{\partial x^2} + L\,\frac{d\xi}{dt} \tag{6}$$

the initial thermal conditions

$$t = 0 : \theta(x) - \theta_0 = 0 \tag{7}$$

and the isothermal boundary conditions

$$x = 0 : \theta(t) - \theta_0 = 0 \tag{8}$$

where $D = \kappa/C$ denotes the thermal diffusivity (κ = conductivity, typical value for concrete: $D = 9 - 10 \times 10^{-7}\ m^2/s$); L = the adiabatic temperature rise according to (4), and θ_0 = the initial temperature. It is instructive to note that the hydration rate $\dot{\xi} = d\xi/dt$ in (2) is homogeneous to the inverse of a time

$$\frac{d\xi}{dt} = \tau_h^{-1} \tag{9}$$

where time τ_h appears as a characteristic time of the hydration reaction. It is considered intrinsic to the material (respectively to the mix-proportions of the material). We introduce some linear transforms of the variables and parameters of the problem:

$$x = Xx'; \quad t = Tt'; \quad \theta - \theta_0 = \Theta(\theta - \theta_0)'; \quad D = \Delta D';$$

$$\tau_h = T_h\tau_h'; \quad L = \Lambda L' \tag{10}$$

Here, x', t', $(\theta - \theta_0)'$, D', τ_h', L' are the dimensionless counterparts of the set of physical quantities x, t, $\theta - \theta_0$, D, τ_h, L of dimension X, T, Θ, Δ, T_h, Λ. The heat equation (6) becomes

$$\frac{\partial(\theta - \theta_0)'}{\partial t'} = \left(\frac{\Delta T}{X^2}\right) D'\,\frac{\partial^2(\theta - \theta_0)'}{\partial x'^2} + \left(\frac{\Lambda}{\Theta}\right) L'\,\frac{d\xi}{dt'} \tag{11}$$

and the kinetics law (9) becomes

$$\frac{d\xi}{dt'} = \left(\frac{T}{T_h}\right)\tau_h^{-1\prime} \tag{12}$$

For the transform set (11) and (12) to satisfy the same equations as the original one, it follows:

$$\frac{\Delta T}{X^2} = \frac{T}{T_h} = \frac{\Lambda}{\Theta} = 1 \tag{13}$$

or equivalently in terms of the invariants of the problem

$$\bar{\xi} = \frac{x}{\sqrt{D\tau_h}} = \frac{x'}{\sqrt{D'\tau_h'}}; \quad \bar{\eta} = \frac{t}{\tau_h} = \frac{t'}{\tau_h'}; \quad \bar{\theta} = \frac{(\theta - \theta_0)}{L} = \frac{(\theta - \theta_0)'}{L'} \tag{14}$$

The solution of the problem is of the self-similar form (Appendix):

$$\bar{\theta} = f\left(\bar{\xi} = \frac{x}{\ell_h}; \quad \bar{\eta} = \frac{t}{\tau_h}\right) \tag{15}$$

This solution reveals the existence of a characteristic length scale ℓ_h, defined by

$$\ell_h = \sqrt{D\tau_h} \tag{16}$$

This gauge-length ℓ_h that relates the thermal diffusivity D (of dimension length^2/time) and a characteristic hydration time τ_h, can be considered a characteristic *hydration heat diffusion length*. To reveal its physical significance, we inspect the heat equation (11) with the following transform:

$$x = \bar{\xi}\ell_h x' \quad \text{with} \quad x' \equiv O(1); \quad t = \bar{\eta}\tau_h t' \quad \text{with} \quad t' \equiv O(1) \tag{17}$$

The heat equation becomes

$$\frac{\partial\bar{\theta}}{\partial t'} = \bar{\eta}\left[\frac{1}{\xi^2}\frac{\partial^2\bar{\theta}}{\partial x'^2} + 1\right] \tag{18}$$

For the semiinfinite half-space ($x > 0$) with zero initial condition ($\theta - \theta_0 = 0$ at $t = 0$), and isothermal boundary condition ($\theta - \theta_0 = 0$ at $x = 0$), (18) has the following asymptotic behavior (Appendix):

$$\bar{\eta}/\bar{\xi}^2 >> 1 : \frac{\partial^2\bar{\theta}}{\partial x'^2} = -\bar{\xi}^2 \tag{19}$$

$$\bar{\eta}/\bar{\xi}^2 << 1 : \frac{\partial\bar{\theta}}{\partial t'} = \bar{\eta} \tag{20}$$

At the time-scale of the hydration reaction, $\bar{\eta} = t/\tau_h \lessapprox O(1)$, the asymptotic behavior reduces to

$$\bar{\xi} << 1 : \frac{\partial^2\bar{\theta}}{\partial x'^2} = 0 \leftrightarrow \bar{\theta} = 0 \tag{21}$$

$$\bar{\xi} >> 1 : \frac{\partial\bar{\theta}}{\partial t'} = \bar{\eta} \leftrightarrow \bar{\theta} = 1 \tag{22}$$

This shows:

- Zones $x << \ell_h$ ($\bar{\xi} << 1$) are locally governed by isothermal conditions; the diffusion is sufficiently intense to ''evacuate'' the latent heat supplied by the hydration process towards the free surface $x = 0$. Given the zero initial condition, there is no significant temperature rise, $\bar{\theta} = 0$.
- On the contrary, for zones $x >> \ell_h$, the diffusion cannot develop in a significant manner [the first term on the right

hand side of (18)] is negligible. Such zones are governed by adiabatic conditions, and the temperature rise is linear in time.

In the above developments, the semiinfinite half-space $x > 0$, and the absence of any specific length scale allowed the hydration-heat diffusion length (16) to be isolated. The structural dimension of heat diffusion $\mathscr{L}$ is the maximum distance of any point within the structure to the nearest isothermal free surface. For $\mathscr{L} >> \ell_h$, main parts of the structure are governed by adiabatic conditions, since they lie in zones far away from the surfaces (with respect to the gauge length ℓ_h). In turn, for $\mathscr{L} << \ell_h$, the structure is sufficiently thin (in comparison with the gauge length) to evacuate the hydration heat through the surface. Inbetween these asymptotic cases, the hydration heat diffusion length, $\ell_h = \sqrt{D\tau_h}$, gives a first estimate whether latent heat affects related to the exothermic nature of the hydration reaction play a role. In other words, the structure is considered ''massive.''

Finally, in the presented derivation $\tau_h = \text{const.}$ was assumed to identify a constant gauge length $\ell_h = \sqrt{D\tau_h}$ defining the size of massive structures. However, the hydration rate $\dot{\xi}$ and its time scale τ_h are defined by kinetics law (2). Comparing (9) and (2), the hydration heat diffusion length can be assessed by

$$\ell_h = \sqrt{D\tau_h(\xi, \theta)} = \sqrt{D\tilde{A}(\xi)^{-1} \exp(E_a/R\theta)} \tag{23}$$

The hydration heat diffusion length hence varies a priori with hydration degree ξ and temperature θ.

Fig. 3 shows ℓ_h as a function of the hydration degree, for the normal strength concrete (NSC), $f_c = 25$ MPa and $w/c = 0.6$) and the high performance concrete (HPC) $f_c = 80$ MPa, $w/c = 0.4$, $s/c = 0.1$) determined from the adiabatic temperature curve of the two materials given in Fig. 1. Fig. 3 shows that ℓ_h is almost constant in the range of hydration degrees $\xi \in [0.1, 0.5]$, in which the maximum adiabatic hydration rate occurs. This justifies the assumption of a constant gauge time $\tau_h(\sim 8-16$ h) in the considered hydration degree range and for adiabatic conditions. In this range, the hydration heat diffusion length is on the order

$$\text{NSC} : \ell_h \simeq 0.3 \text{ m}; \quad \text{HPC} : \ell_h \simeq 0.2 \text{ m} \tag{24}$$

The values indicate that HPC structures are, in general, more sensitive to hydration heat effects than NSC structures, as a result of the higher hydration rate (respectively lower characteristic hydration time τ_h) of HPC. However, what is most remarkable is that the values determined by means of dimensional analysis almost perfectly agree with the rich body of experience acquired on sites of large-scale civil engineering concrete projects (Acker and Ulm 2000). Thermal effects are very small for NSC structural elements, as long as $2\mathscr{L} < 2 \times 0.3$ m, and for HPC structural elements as long as $2\mathscr{L} < 2 \times 0.2$ m (the factor 2 is a structural element that is cooled from both sides). Conversely, as soon as there is a zone of concrete more than $2\mathscr{L} = 0.6$ m for NSC and more than $2\mathscr{L} = 0.4$ m for HPC from the nearest cooled surface, the temperature of the concrete will rise by 30–50 K in NSC and even 55 K in HPC structures. Cracking in the course of cooling is then practically inevitable.

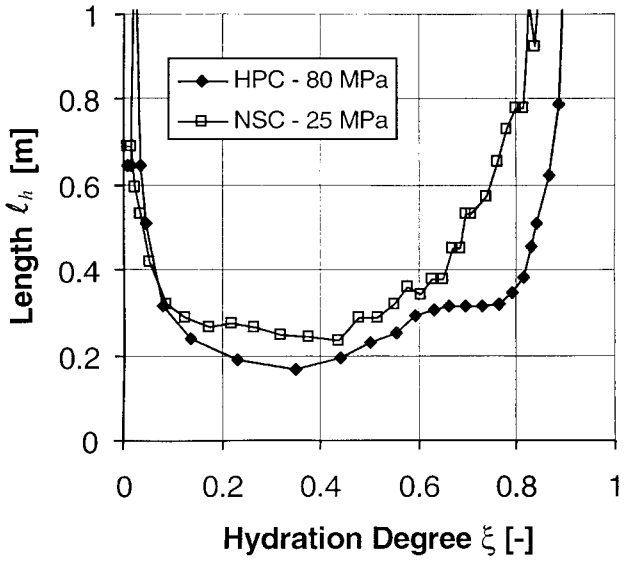

FIG. 3. Hydration Heat Diffusion Length as Function of Hydration Degree for High Performance Concrete (HPC) and a Normal Strength Concrete (NSC)

THERMO-CHEMO-MECHANICS OF EARLY-AGE CONCRETE STRUCTURES

Early-age concrete structures are considered as ''massive'' when the structural dimension $\mathscr{L}$ of heat diffusion exceeds the hydration heat diffusion length ℓ_h defined by (23). Typical massive structures are concrete dams, concrete foundations, high-rise building concrete columns, large span bridge girders, etc., for which hydration heat effects can be critical for the risk of early-age concrete cracking. The risk of early-age concrete cracking depends on the capacity of hardening concrete to support the thermal stresses caused by the exothermic nature of the hydration process; a competition between stress and strength development takes place. The prediction and limitation of this early-age concrete cracking is important to ensure the long-term structural integrity of concrete structures. The Finite Element Method, in combination with an efficient time integration scheme for the governing rate equations, is well suited for this purpose (Hellmich et al. 1999b; Sercombe et al. 2000).

Length-Time Scales of Finite Element Simulation of Early-Age Concrete Structures

The analysis of early-age concrete structures requires: (1) an appropriate finite element discretization of both the hydrating concrete and of the thermal boundary conditions; and heat exchange conditions through the formwork and free surfaces of the structure. A realistic simulation of curing conditions, partial formwork removal, concrete joints, detailed concreting and casting cycles is needed (Ulm 1996). These construction stages represent a change in thermal and mechanical boundary conditions.

In general, the hydrating bulk material is modeled by means of solid elements. The time step Δt of the integration of the heat equation needs to be adapted to the solid element size. Employing similar dimensional arguments, as in the 1D case for the diffusion finite element size, it is

$$\Delta t \leq \frac{\ell^2}{D} < \frac{\ell_h^2}{D} \tag{25}$$

where ℓ is the smallest solid finite element size in the mesh.

The outgoing heat flux $\mathbf{q}\cdot\mathbf{n}$ through typical formworks employed in concrete applications (wood, steel (sometimes) insulated with polyurethane foam layers) is suitably modeled by a linear exchange condition through the surface Γ oriented by unit normal $\mathbf{n}$

$$\text{at } \Gamma\text{: } \mathbf{q}\cdot\mathbf{n} = \kappa\nabla(\theta - \theta_0)\cdot\mathbf{n} = -\kappa\frac{\partial(\theta - \theta_0)}{\partial s} = \lambda(\theta - \theta_s) \tag{26}$$

where θ_s = the external surface temperature; κ = the conduc-

TABLE 1. Exchange Coefficient λ for Common Surfaces and Formworks (Ulm 1996).

Type of surface	λ[kJ/h/m²/K] Ventilated	Non-ventilated
Free surface (air)	21.6	14.4
Steel form (2 mm)	19.6	14.4
Wood form (20 mm)	11.2	9.2
Concreting foil	1.8–3.6	
Polyurethane insulator (50 mm)	1.55	

tivity; and $\partial\theta/\partial s$ = the normal temperature gradient at the boundary Γ. The exchange coefficient λ depends on the type of formwork and air ventilation conditions. Table 1 gives the mean values of exchange coefficients measured for typical formworks and curing conditions employed in concrete applications. (Recall that the conductivity κ has dimensions of energy/time × length × temperature; and exchange coefficient λ has dimensions of energy/time × length² × temperature.) Note κ/λ has the dimension of length that introduces another length scale in the problem. If the following set of linear transforms are introduced

$$s = Ss'; \quad \kappa = K\kappa'; \quad \lambda = L\lambda'; \quad (\theta - \theta_0) = \Theta(\theta - \theta_0)';$$
$$(\theta_0 - \theta_s) = \Theta_s(\theta_0 - \theta_s)' \tag{27}$$

(26) reacts in the dimensionless form

$$\text{at } \Gamma: \ -\frac{\partial(\theta - \theta_0)'}{\partial s'} = \left(\frac{S}{K/L}\right)\frac{\lambda'}{\kappa'}\left[\frac{\Theta_s}{\Theta}(\theta_0 - \theta_s)' + (\theta - \theta_0)'\right] \tag{28}$$

Dimensional homogeneity of the boundary condition (26) and (28) requires

$$\frac{S}{K/L} = \frac{\Theta_s}{\Theta} = 1 \tag{29}$$

or equivalently

$$\frac{s}{\kappa/\lambda} = \frac{s'}{\kappa'/\lambda'}; \quad \frac{\theta - \theta_0}{\theta_0 - \theta_s} = \frac{(\theta - \theta_0)'}{(\theta_0 - \theta_s)'} \tag{30}$$

The first invariant, the heat exchange length κ/λ defines a boundary layer, in which the effects of the heat exchange condition (26) are appreciable. Small values of κ/λ correspond to low heat retaining formworks (steel form, free ventilated surface), while large values of κ/λ approach the zero flux through the boundary. From a practical point of view of finite element meshing, this length scale needs to be considered, in addition to the hydration heat diffusion length ℓ_h [(25)]. The solid diffusion elements in the vicinity of the exchange elements must be of a characteristic length much smaller than κ/λ.

Optimization Criterion for Massive Structures

The first case study focuses on thermo-chemical couplings in massive concrete structures. It is part of a feasibility study devoted to the structural optimization of tunnel platforms for high-speed trains made of steel-fiber reinforced (SFR) HPC. Several configurations were studied; two are illustrated in Fig. 4. The solution in Fig. 4(a) consists of a plain concrete platform cast-in-place on existing ballast. The composite solution shown in Fig. 4(b) consists of reversed U-profiled precast RC beams, empty to the inside and covered by cast-in-place SFR-HPC to the outside. The 0.5 m thickness of the platform was required to ascertain a sufficiently high eigenfrequency with regard to the excitation frequency of the high-speed trains running on the tunnel platform.

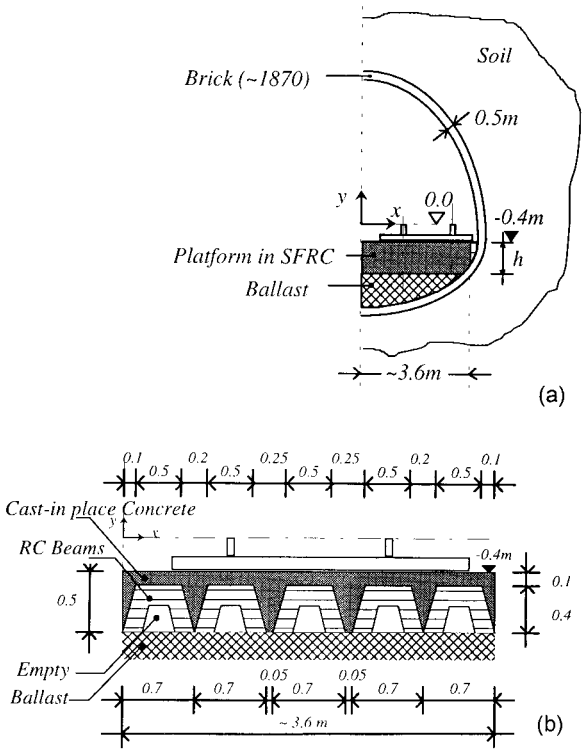

FIG. 4. Structural Platform Solutions: (a) Plain Concrete; and (b) U-Profiled Precast RC Beams Covered by Cast-in-Place Fiber Reinforced Concrete

This case study is well suited to develop a design criterion for massive concrete structures.

Structural Thermo-Chemical Couplings

For the two structural configurations, temperature and hydration degree were determined by means of 2D thermo-chemical finite element simulations. Fig. 5(a) shows the results, in terms of the normalized temperature rise $(\theta(t) - \theta_0)/L$ versus the hydration degree $\xi(t)$ at the location corresponding to the highest temperature rise in the structure. Both temperature and hydration degree are direct results of the finite element simulation. The bisecting line $x = y$ corresponds to adiabatic conditions [when neglecting the first term on the right hand side of (1)], while the horizontal line corresponds to isothermal conditions $\theta - \theta_0 = 0$. The results show a quasi-adiabatic behavior of the plain, concrete, platform solution up to high hydration degrees, the U-profile composite solution exhibits a smaller temperature rise, and the cooling starts at smaller hydration degrees. This improved structural performance results from the structural capacity of the U-profile composite solution to ''evacuate'' the latent hydration heat by means of diffusion to the outside. Fig. 5(b) shows the normalized heat transferred by conduction, $Q(t)/L = -1/L \int_0^t \nabla \cdot \mathbf{q}\, dt$, versus the hydration degree $\xi(t)$ at the location corresponding to the temperature developments of Fig. 5(a). The bisecting line $Q/L = \xi$ corresponds to the ideal case of isothermal conditions [$\partial\theta/\partial t = 0$ in (1)], while the horizontal axis corresponds to adiabatic conditions, $Q° = 0$. From these analyses of thermo-chemical couplings at a structural level, the U-profile solution can be considered optimized in terms of its structural heat diffusivity capacity (Ulm and Coussy 1998). From a mechanical point of view, the effect of this optimized structural heat transport capacity is two-fold. A smaller temperature rise is associated with a lower stress intensity generated by restrained thermal expansion (heating phase) and shrinkage (cooling phase). In addition, a low hydration degree at the onset of cooling is critical to reduce the risk of early-age concrete

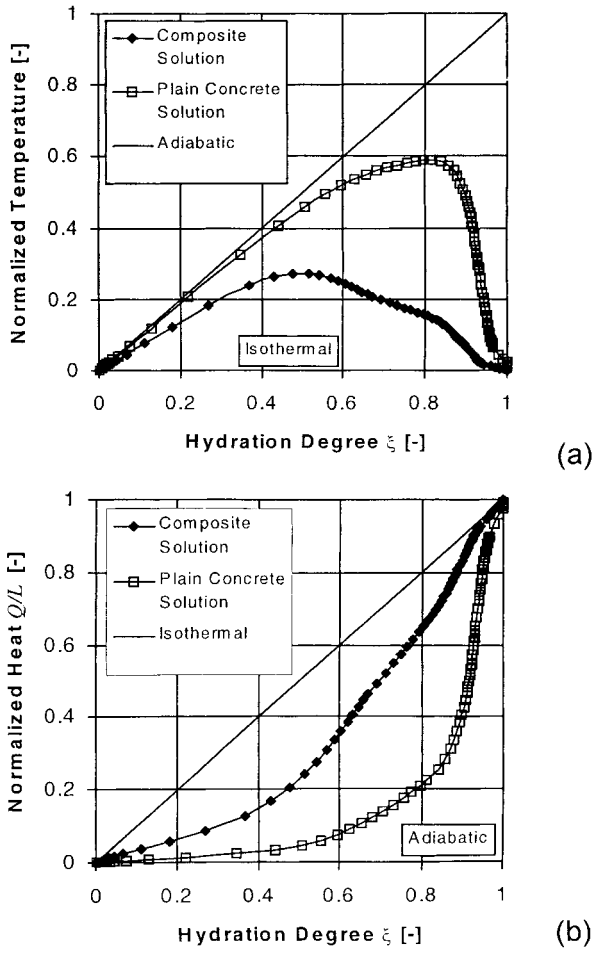

FIG. 5. Structural Thermo-Chemical Couplings: (a) Normalized Temperature; and (b) Normalized Heat versus Hydration Degree

cracking. The lower the hydration degree at the onset of cooling, the smaller the stiffness of the material, and the lower the tensile stresses generated by restrained thermal shrinkage.

Key Design Parameters of Massive Concrete Structures

To quantify this optimized structural performance and to seek the governing design parameters the integrated form of the 3D heat equation in the fresh poured concrete volume Ω is written in the form

$$\frac{\kappa}{D}\int_{\Omega}\left(\frac{\partial(\theta-\theta_0}{\partial t}-L\frac{d\xi}{dt}\right)d\Omega=-\int_{\Omega}\nabla\cdot\mathbf{q}\,d\Omega \tag{31}$$

Substituting $\dot{\xi}=\tau_h^{-1}$ and using the divergence theorem and the linear exchange condition (26), (31) becomes

$$\frac{\kappa}{D}\int_{\Omega}\left(\frac{\partial(\theta-\theta_0)}{\partial t}-\frac{L}{\tau_h}\right)d\Omega=\lambda\int_{\Gamma}[(\theta-\theta_0)+(\theta_0-\theta_s)]\,d\Gamma \tag{32}$$

where, for purpose of analysis, a constant exchange coefficient λ for the heat exchange through boundary Γ is considered. Some linear transform of the variables and parameters of the problem are now introduced:

$$t=T_h t';\quad \tau_h=T_h\tau_h';\quad d\Omega=X^3\,d\Omega';\quad d\Gamma=X^2\,d\Gamma';$$
$$\kappa=K\kappa';\quad D=\Delta D';\quad \lambda=L\lambda' \tag{33}$$

$$L=\Lambda L';\quad (\theta-\theta_0)=\Theta(\theta-\theta_0)';\quad (\theta_0-\theta_s)=\Theta_s(\theta_0-\theta_s)' \tag{34}$$

Eq. (34) accounts for a difference between the concrete placing temperature θ_0 and the outside temperature θ_s. This was not considered in the transform set of the 1D problem (10). Eqs. (32), (33) and (34) yield

$$\frac{\kappa'}{D'}\int_{\Omega'}\left[\frac{\partial(\theta-\theta_0)'}{\partial t}-\frac{\Lambda}{\Theta}\frac{L'}{\tau_h'}\right]d\Omega'=\left(\frac{\Delta T_h}{XK/L}\right)$$
$$\cdot\lambda'\int_{\Gamma'}\left((\theta-\theta_0)'+\frac{\Theta_s}{\Theta}(\theta_0-\theta_s)'\right]d\Gamma' \tag{35}$$

The transform set satisfied the same equations as the original one provided that

$$\frac{\Delta T_h}{XK/L}=\frac{\Lambda}{\Theta}=\frac{\Theta_s}{\Theta}=1 \tag{36}$$

Therefore, the normalized temperature rise $\bar{\theta}=(\theta-\theta_0)/L$ will be governed by the values of invariants of similarity parameters

$$\bar{\theta}_s=\frac{\theta_0-\theta_s}{L};\quad \bar{\xi}=\frac{\Gamma}{\Omega}\frac{\ell_h^2}{\kappa/\lambda} \tag{37}$$

These invariants or similarity parameters are as follows.

- The normalized surface-to-placing temperature invariant θ_s reflects the well-known effect of thermal curing on the temperature rise in massive structures. It is the difference between placing temperature θ_0 and surface temperature θ_s, normalized by the latent heat of hydration L, which needs to be considered when optimizing the thermal curing conditions (surface heating or cooling). For typical values of L, the thermal treatments are more efficient for normal strength concretes with moderate cement contents (typically $c\simeq 300$ kg/m^3) leading to moderate hydration heat production ($L\simeq 40$ K), than for high performance concretes (typically $c\simeq 400$ kg/m^3, $L\simeq 60$ K).
- The structural heat transport capacity, expressed by invariant ξ, is affected by three parameters: (1) the surface-to-volume ratio Γ/Ω; (2) the heat exchange length k/λ; and (3) the hydration heat diffusion length ℓ_h. The surface-to-volume ratio Γ/Ω is a structural design parameter and has been optimized in the case study of the tunnel platform. The heat exchange length κ/λ is related to the choice of formwork. Finally, the hydration heat diffusion length ℓ_h of massive concrete structures, and the characteristic hydration time τ_h require appropriate material design for a given structure. Specifically, concrete with less ''nervous'' cements (low hydration rate) are more appropriate for hydration heat sensitive concrete structures.

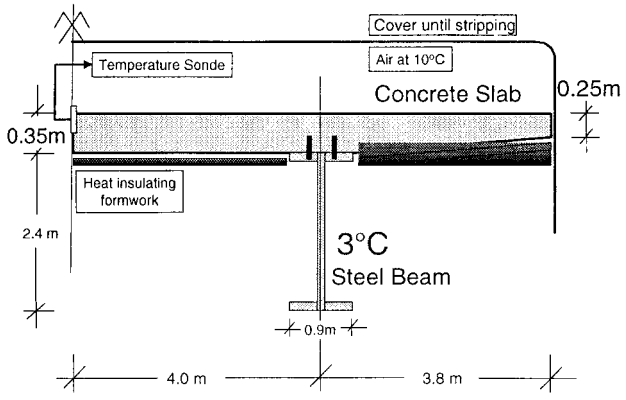

FIG. 6. Concrete-Steel Composite Bridge Casted in Winter

Due to physical similarity (Buckingham 1914; Barenblatt 1996; Sonin 1997), these parameters can be used to monitor the temperature rise in ''massive'' concrete structures. For instance, if we consider structures 1 and 2 with different materials ($L_1 \neq L_2$; $\ell_{h1} \neq \ell_{h2}$), different geometries ($\Gamma_1/\Omega_1 \neq \Gamma_2/\Omega_2$), and different initial and boundary conditions ($\theta_{01} \neq \theta_{02}$; $\theta_{s1} \neq \theta_{s2}$; $\lambda_1 \neq \lambda_2$), the normalized temperature rise θ in both structures will be the same. The governing invariants θ_s and ξ in both structures have exactly the same values

$$\bar{\theta} = \frac{(\theta - \theta_0)_1}{L_1} = \frac{(\theta - \theta_0)_2}{L_2} = F\left(\bar{\theta}_s = \frac{(\theta_0 - \theta_s)_1}{L_1} = \frac{(\theta_0 - \theta_s)_2}{L_2};\right.$$

$$\left.\bar{\xi} = \frac{\Gamma_1}{\Omega_1}\frac{\ell_{h1}^2}{(\kappa/\lambda)_1} = \frac{\Gamma_2}{\Omega_2}\frac{\ell_{h2}^2}{(\kappa/\lambda)_2}\right) \tag{38}$$

where subscripts 1 and 2 designate the structre. Eq. (38) can be considered a structural similarity criterion for scaling the structural performance of massive early-age concrete structures.

Stripping Time Criterion for Winter Concreting

Stripping time is the time elapsed between concreting and formwork removal. Short stripping times are essential for an efficient construction management. From a chemo-mechanical perspective, the stripping time is the time required for the structural material to develop the necessary load bearing capacity of the structural element in the moment of formwork removal. This depends on material stiffness, strength development, and the hydration progress within the concrete structure. The problem involves chemo-mechanical couplings between: (1) the hydration progress, stiffness and strength development; and (2) structural load bearing capacity.

The structure considered here is a concrete-steel composite bridge. This type of bridge is commonly employed for bridges with medium spans up to 80 m. The structure is shown in Fig. 6. It is composed of a concrete deck, 0.35 m thick in the center and 0.25 m at the edges. The concrete deck of 8.0 m span and 3.8 m cantilever is carried by two steel beams. For this case study, a typical two-phase construction associated with different thermal and mechanical boundary conditions was considered. *Before stripping* the dead-load is carried by the formwork and by the flanges of the steel beams. The bridge deck is protected by a cover with an air ventilation at $\theta_s = 10$°C. The formwork is heat insulated (by means of polyurethane foam layers), but the steel-flange is not. It is in contact with the winter environment at a mean temperature of $\theta_s = 3$°C. The placing temperature of concrete is $\theta_0 = 10$°C. *After formwork removal*, the concrete deck carries the dead-load to the supports formed by the steel beam flanges. Both upper and lower surfaces are in contact with the mean winter air temperature of 3°C.

Temperature Development

The structure before stripping is rather ''massive'' ($\ell_h/\mathcal{L} \leq 1$). Due to the heat insulating formwork ($\kappa/\lambda = 1.6$ m), the heat in the structure mainly escapes through the protected deck surface ($\kappa/\lambda = 0.25$ m). The structural dimension of heat diffusion $\mathcal{L}$ is then approximately equal to the element thickness, and $\ell_h/\mathcal{L} \leq 1$ (recall $\ell_h \sim 0.2 - 0.3$ m). In turn, after formwork removal, both upper and lower surfaces are in direct contact with the environmental temperature ($\kappa/\lambda = 0.32$ m). The structural dimension of heat diffusion $\mathcal{L}$ becomes approximately equal to half of the element thickness, and thus, $\ell_h/\mathcal{L} \geq 2$. The structure can be considered as slender. Fig. 7 illustrates this switch from a heat sensitive ($\ell_h/\mathcal{L} \equiv 1$) to a heat insensitive structure ($\ell_h/\mathcal{L} > 1$) at stripping time $t_0 = 24$ h at which cooling starts. The figure shows the *in situ* measurements of the temperature developments in the center of the bridge deck (axis of symmetry). It also shows the results of temperature against time in the center and on the surface of the bridge deck obtained by means of the finite element method.

The results agree quite well with the *in situ* data in both amplitude and kinetics in the hours after pouring. In return, the results show that changes in stripping time do not significantly change the overall temperature development. For instance, for a form removal at $t_0 = 16$ h, a maximum difference in temperature rise of $\Delta\theta = 5$ K can be expected. This is too small to significantly affect the mechanical behavior, and serve as form removal criterion for the considered concreting situation in winter.

A Chemo-Mechanical Form Removal Criterion

We now turn to the risk of early-age concrete cracking of the structure with regard to different times of form removal at $t_0 = 16$ h, $t_0 = 24$ h and $t_0 = 30$ h. In a first approach, a chemoelastic analysis is performed (Coussy 1995; Ulm and Coussy 1996):

$$\xi \geq \xi_0\text{: } d\sigma_{ij} = \left(K(\xi) - \frac{2}{3}G(\xi)\right)d\epsilon\delta_{ij} + 2G(\xi)d\varepsilon_{ij}$$

$$- 3[\alpha K(\xi)d\theta - \beta K_\infty d\xi]\delta_{ij} \tag{39}$$

where ξ_0 is the so-called percolation threshold of the solidi-

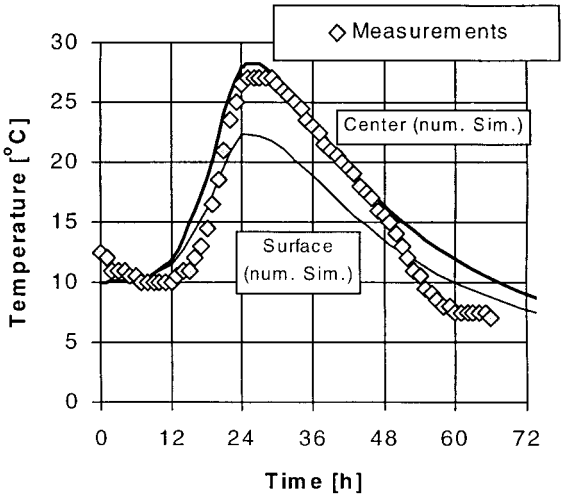

FIG. 7. Temperature Development: Comparison of On-Site Recorded Temperatures, and Results Obtained by Finite Element Simulations

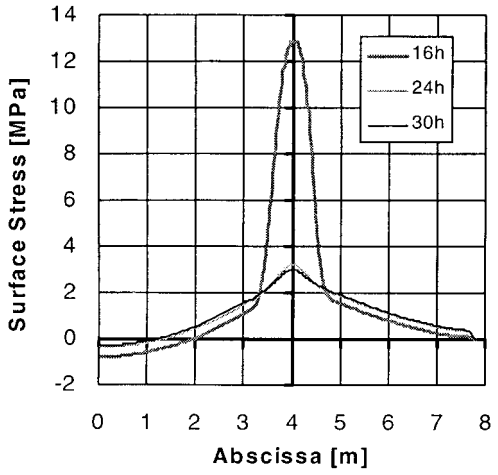

FIG. 8. Chemoelastic Surface Stresses for Different Stripping Times

fying material, the hydration degree beyond which fresh concrete can support a stress deviator (Acker 1988); $K(\xi)$ and $G(\xi)$ represent the bulk modulus and shear modulus that depend on the hydration degree ξ (Byfors 1980; Boumiz et al. 1995); K_∞ is the asymptotic bulk modulus of the hardened material; $\epsilon = \varepsilon_{ij}\delta_{ij}$ is the volume strain; ε_{ij} is the strain tensor; δ_{ij} is the Kronecker delta; α is the thermal dilatation coefficient; and β is the chemical dilatation coefficient, which accounts for autogenous shrinkage. The derivation of (39) and the experimental determination of the different material parameters go beyond the scope of this paper. The theoretical foundations can be found in Coussy (1995) and Coussy and Ulm (1996); and the application to concrete can be found in Ulm and Coussy (1996), Hellmich et al. (1999a), and Sercombe et al. (2000).

In Fig. 8 the transversal stresses σ_{xx} along the top-fiber of the section under dead-load in the moment of formwork removal for different stripping times are given. There is a significant difference in stress distribution along the surface with a (chemoelastic) stress excess at the support for a form removal at t_0 = 16 h, which largely exceeds the tensile strength of the material. On closer look, this stress excess can be ex-

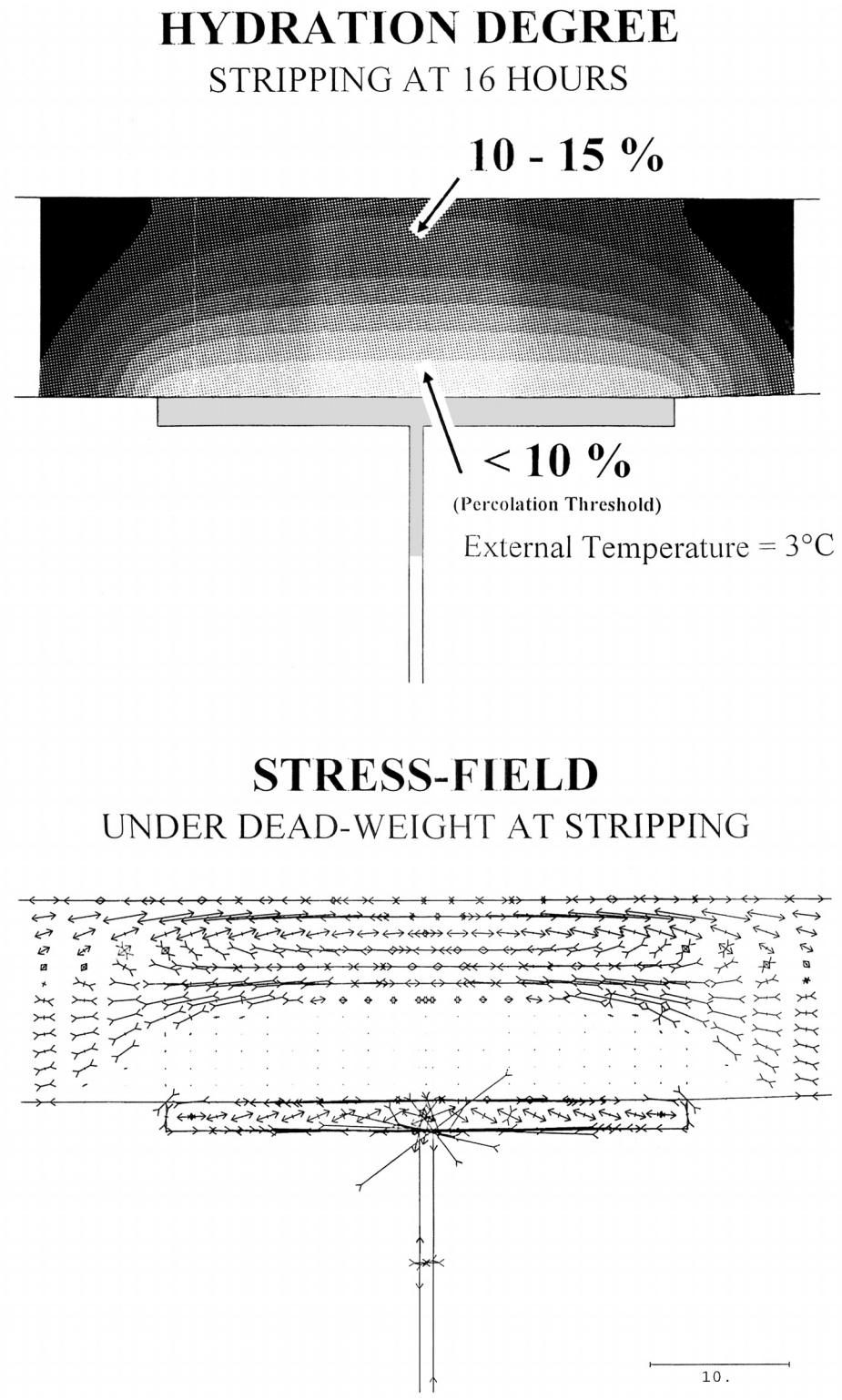

FIG. 9. Stripping at 16 h: Hydration Degree and Associated Stress Field

plained as an hydration kinetics effect on the mechanical stress distribution in the moment of form removal. For the form removal at t_0 = 16 h, Fig. 9 gives the fields of hydration degree and stresses in the concrete element in contact with the steel section. The figure shows that the hydration degree is inferior to the percolation threshold ξ_0 in more than half of the section in direct contact with the steel beam exposed to the outside temperature of 3°C. This spatial hydration degree distribution results from the thermal activation of the hydration reaction. Due to the lower temperature, the hydration reaction progresses at a very low rate and does not exceed the percolation threshold in the 16 h stripping time. The mechanical implication is that half of the section below the percolation threshold has neither an elastic stiffness nor a material strength to support the stresses generated at the support by the dead-load at stripping (Fig. 9). Only half of the section is active in a mechanical sense, which leads to the stress excess for a stripping time t_0 = 16 h. It constitutes a chemo-mechanical cross-effects at the structural level of the composite bridge. It becomes clear when comparing these results with those obtained for a stripping at t_0 = 30 h, shown in Fig. 10. The hydration degree in the entire section is beyond the percolation thresh-

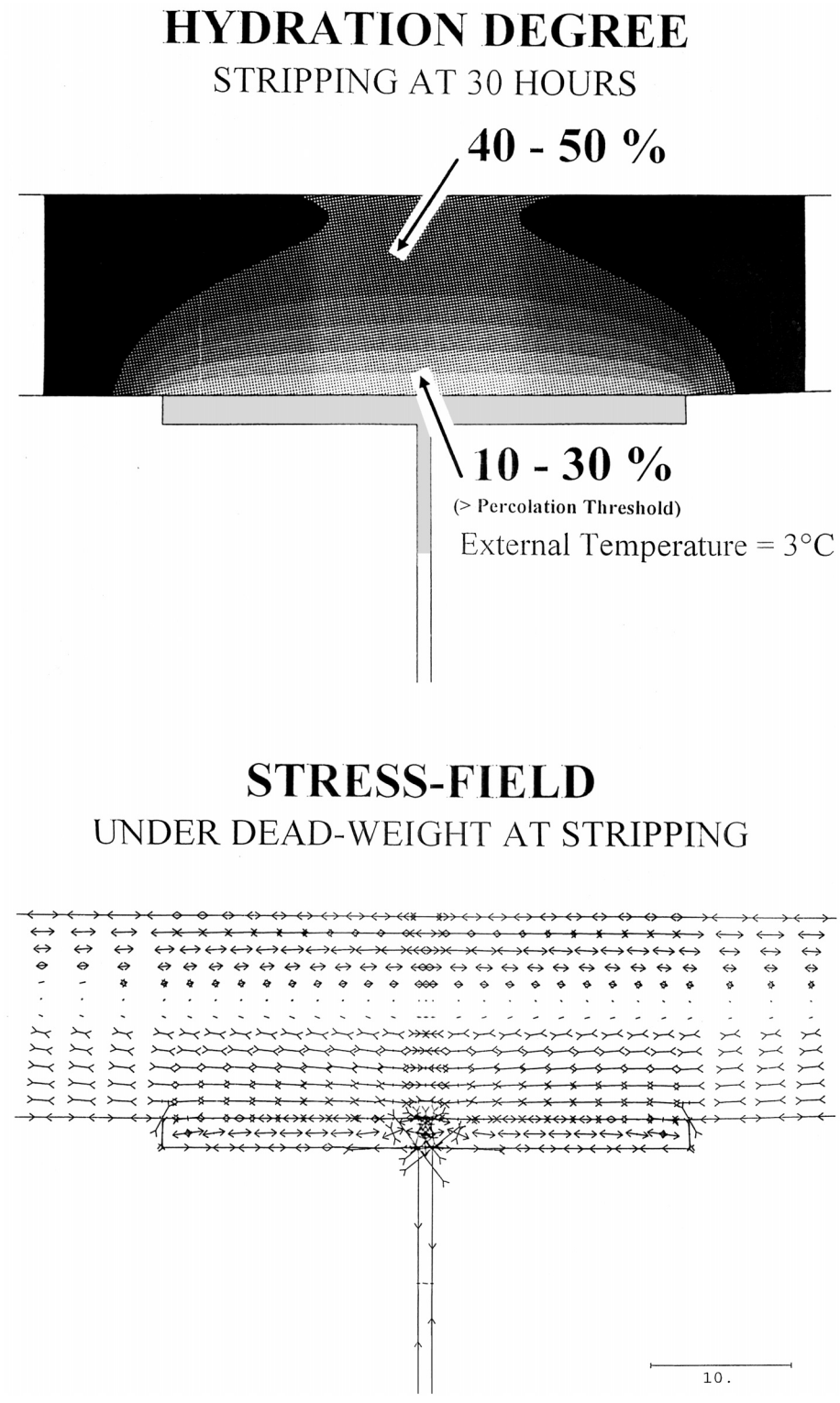

FIG. 10. Stripping at 30 h: Hydration Degree and Associated Stress Field

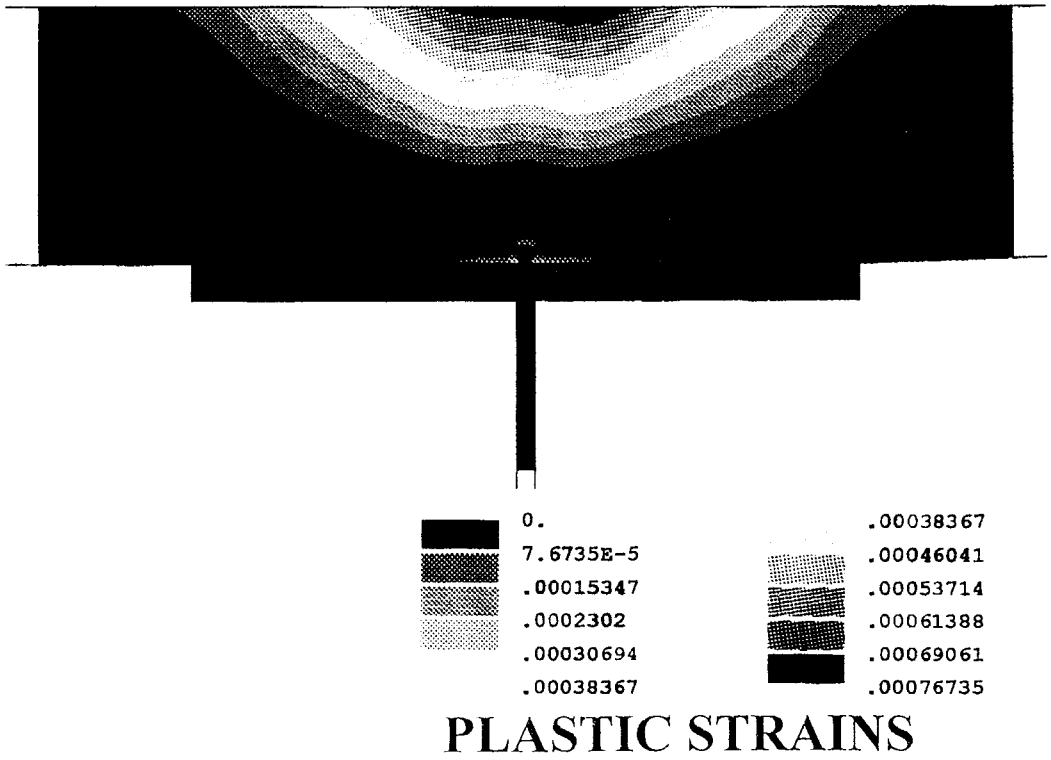

FIG. 11. Contours of Plastic Strains at Support for Stripping at 24 h

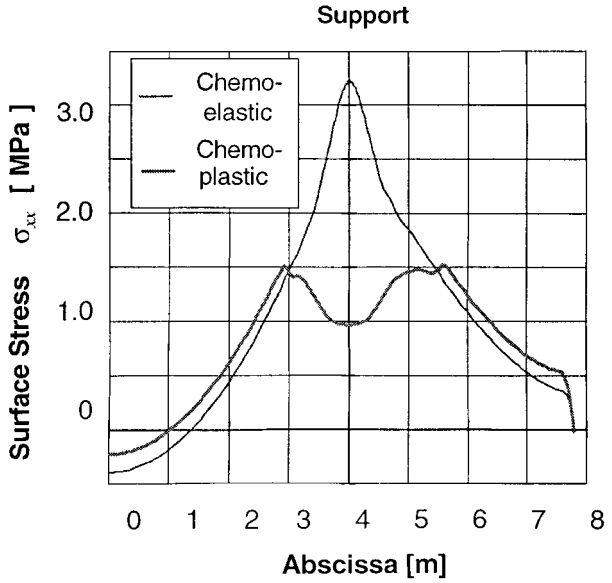

FIG. 12. Chemoelastic and Chemoplastic Transversal Surface Stresses for Stripping at 24 h

old, allowing for a complete stress distribution over the entire mechanically active section at form removal.

The chemoelastic analysis can be completed with a chemoplastic one (Ulm and Coussy 1996; 1998; Hellmich et al. 1999):

$$\xi \geq \xi_0: d\sigma_{ij} = \left(K(\xi) - \frac{2}{3}G(\xi)\right)(d\epsilon - d\epsilon^p)\delta_{ij} + 2G(\xi)(d\varepsilon_{ij} - d\varepsilon_{ij}^p) - 3[\alpha K(\xi)d\theta + \beta K_\infty d\xi]\delta_{ij} \quad (40)$$

The plastic criterion is the 3-parameter Willam-Warnke criterion (Willam and Warnke 1975) with chemical hardening (Ulm et al. 1998). There exists no equilibrium path within the strength domain of early-age concrete for a stripping time t_0 = 16 h. The chemoelastic stress excess may entail a blunt fracture at support, which can lead to structural failure. The chemoplastic analysis is limited to stripping at 24 hours. The risk of cracking can be evaluated in terms of plastic strains ε_{ij}^p shown in Fig. 11. Transversal stresses at the top fibers are given in Fig. 12. The microcracking at support leads to a redistribution of stresses reducing the stresses in weaker parts (support) to the stiffer ones. This kind of redistribution can be considered as measurement for a good structural performance at stripping after 24 h.

CONCLUSIONS

The invariants or similarity parameters, identified by means of dimensional analysis, allow monitoring of the structural performance of early-age concrete structures.

1. The hydration heat diffusion length ℓ_h is a material to structural key design parameter for the quantification of the hydration heat sensitivity of early-age concrete structures. The smaller the more ''nervous'' the concrete mix. For a given structural dimension $\mathcal{L}$, there is an a priori higher risk of early-age concrete cracking of HPC structures.
2. For a given concrete mix, defined by the hydration heat diffusion length ℓ_h, the risk of early-age concrete cracking can be efficiently reduced by simultaneously increasing the structure's surface to volume ratio Γ/Ω and reducing the heat exchange length κ/λ through an appropriate choice of formwork (Table 1). Based on physical similarity, a careful design of these different length scales can ensure an optimized, structural heat, diffusivity capacity.
3. For winter pouring of ''thin'' concrete structures, the temperature history and the hydration progress in the entire structure need to be considered. Local effects of thermoactivation of the hydration rate may impair the structural stability at formwork removal. The unique features of thermo-chemo-mechanical finite element analysis pro-

vide assistance to predict and reduce the risk of early-age concrete cracking. Implemented in commercially available finite element packages, these model-based simulation tools can become a key component of on-line decision support systems for construction processes. The similarity parameters identified in this paper will serve as gauge-length and gauge-time of model-based design optimization.

ACKNOWLEDGMENTS

This research was conducted as part of a cooperation between the Laboratoire Central des Ponts et Chaussées, Paris, and the Massachusetts Institute of Technology. The financial support by LCPC and the Gilbert W. Winslow Career Development Chair at MIT is gratefully acknowledged. The case studies in this paper were obtained with the finite element program CESAR-LCPC during the professional involvement of the first writer at LCPC (1990–98). We gratefully acknowledge the technical support of the CESAR-LCPC development team through Jacques Oczkowski and Dr. Pierre Humbert, for installation and maintenance of CESAR-LCPC@MIT.

APPENDIX. ASYMPTOTIC BEHAVIOR OF 1D-HEAT DIFFUSION EQUATION WITH CONSTANT SOURCE TERM

The solution to the 1D-heat diffusion (6), initial and boundary conditions (7) and (8), and kinetics law (9) is the self-similar solution

$$\bar{\theta} = f\left(\bar{\xi} = \frac{x}{\ell_h};\quad \bar{\eta} = \frac{t}{\tau_h}\right) = \bar{\eta}\left(1 - 4i^2\left[1 - \operatorname{erf}\left(\frac{\bar{\xi}}{2\sqrt{\bar{\eta}}}\right)\right]\right) \tag{41}$$

where

$$\operatorname{erf} y = \frac{2}{\sqrt{\pi}}\int_0^y \exp(-z^2)\,dz \quad \text{and} \quad i^n f(z) = \int_z^\infty i^{n-1} f(u)\,du$$

An asymptotic expansion of this solution reads:

$$\bar{\xi} << \sqrt{\bar{\eta}} : \frac{\theta - \theta_0}{L} \equiv \frac{2}{\sqrt{\pi}}\bar{\xi}\sqrt{\bar{\eta}} \tag{42}$$

$$\bar{\xi} >> \sqrt{\bar{\eta}} : \frac{\theta - \theta_0}{L} \equiv \bar{\eta} \tag{43}$$

which for $\bar{\eta} \lessapprox O(1)$ leads to (21) and (22).

REFERENCES

Acker, P. (1988). ''Mechanical behavior of concrete: A physico-chemical approach.'' *Res. Rep., LPC 152* Laboratoires des Ponts et Chaussées, Paris (in French).

Acker, P., and Ulm, F.-J. (2000). ''Creep and shrinkage of concrete: Physical origins and practical measurements.'' *Nuclear Engrg. and Des.*, in press.

Barenblatt, G. I. (1996). *Scaling, selfsimilarity, and intermediate asymptotics*, Cambridge Texts in Applied Mathematics, Cambridge University Press, Cambridge, U.K.

Boumiz, A., Vernet, C., and Tanoudji, C. F. (1996). ''Mechanical properties of cement pastes and mortars at early ages: Evolution with time and degree of hydration.'' *Advn. Cement. Bas. Mat.*, 3, 92–106.

Buckingham, E. (1914). ''On physically similar systems: Illustrations of the use of dimensional analysis.'' *Phys. Rev.*, 4, 345–376.

Byfors, J. (1980). ''Plain concrete at early ages.'' *Res. Rep., F3:80*, Swedish Cement and Concrete Res. Inst., Stockholm.

Cervera, M., Oliver, J., and Prato, T. (1999). ''Thermo-chemo-mechanical model for concrete. I: Hydration and aging.'' *J. Engrg. Mech.*, ASCE, 125(9), 1018–1027.

Coussy, O. (1995). *Mechanics of porous continua*, Wiley, Chichester, U.K.

Coussy, O., and Ulm, F.-J. (1996). ''Creep and plasticity due to chemo-mechanical couplings.'' *Archive of Appl. Mech.*, 66, 523–535.

Hellmich, C., Ulm, F.-J., and Mang, H. A. (1999a). ''Multisurface chemo-plasticity. I: Material model for shotcrete.'' *J. Engrg. Mech.*, ASCE, 125(6), 692–701.

Hellmich, C., Ulm, F.-J., and Mang, H. A. (1999b). ''Consistent linearization in finite element analysis of coupled chemo-thermal problems with exo- or endothermal reactions.'' *Computational Mech.*, 24(4), 238–244.

Powers, G., and Brownyard, T. L. (1948). ''Studies of the physical properties of hardened Portland cement paste.'' *Res. Bull. 22*, Portland Cement Association, Skokie, Ill.

Sercombe, J., Hellmich, C., Ulm, F.-J., and Mang, H. (2000). ''Modeling of early-age creep of shotcrete. I: Model and model parameters.'' *J. Engrg. Mech.*, ASCE, 126(3), 284–291.

Sercombe, J., Ulm, F.-J., and Mang, H. A. (2000). ''Consistent return mapping algorithm for chemoplastic constitutive laws with internal couplings,'' *Int. J. Numer. Methods in Engrg.*, 47, 75–100.

Sonin, A. A. (1997). *The physical basis of dimensional analysis*. Dept. of Mech. Engrg., Massachusetts Institute of Technology, Cambridge, Mass.

Ulm, F.-J., and Coussy, O. (1995). ''Modeling of thermochemomechanical couplings of concrete at early ages.'' *J. Engrg. Mech.*, ASCE, 121(7), 785–794.

Ulm, F.-J. (1996). ''Modélisation du béton au jeune âge (Modeling of concrete at early ages.'' *CESAR-LCPC 3.2: Program Manuel*, 3rd Ed., LCPC, Paris (in French).

Ulm, F.-J., and Coussy, O. (1996). ''Strength growth as chemo-plastic hardening in early age concrete.'' *J. Engrg. Mech.*, ASCE, 122(12), 1123–1132.

Ulm, F.-J., and Coussy, O. (1998). ''Couplings in early-age concrete: From material modeling to structural design.'' *Int. J. Solids and Struct.*, 35(31–32), 4295–4311.

Ulm, F.-J., Coussy, O., and Hellmich, C. (1998). ''Chemoplasticity: A review of evidence.'' *Computational modelling of concrete structures*, R. de Borst, N. Bicanic, H. Mang, and G. Meschke, eds., Balkema, Rotterdam, The Netherlands, 421–439.

Willam, K. J., and Warnke, E. P. (1975). ''Constitutive model for the triaxial behavior of concrete.'' *IABSE Proc., 19, Seminar on concrete structures subjected to triaxial stresses, Paper III-1*, International Association for Bridge and Structural Engineering, Zurich.

NOTATION

The following symbols are used in this paper:

$\tilde{A}$ = normalized affinity;
C = volume heat capacity;
c = cement mass per unit volume;
D = thermal diffusivity;
E_a = activation energy;
F = dimensionless function;
f_c = compression strength (28 days);
G = shear modulus;
K, K_∞ = bulk modulus, asymptotic bulk modulus;
K = dimension function of κ;
L = adiabatic hydration temperature rise;
$\mathscr{L}$ = structural dimension of heat diffusion;
L = dimension function of λ;
l = latent heat of hydration;
ℓ = characteristic finite element mesh size;
ℓ_h = hydration heat diffusion length;
m_{sk}, $m_{sk}(\infty)$ = hydrate mass; asymptotic hydrate mass;
n = outward unit normal;
$O(1)$ = order of 1;
Q = external heat supply;
q = heat flux vector;
R = universal gas constant;
s/c = silica fume to cement ratio;
T = dimension function of t;
T_h = dimension function of τ_h;
t = time;
t_0 = stripping time;
w/c = water-cement ratio;
X = dimension function of x;
x = space coordinate;
α = thermal dilatation coefficient;
β = chemical dilatation coefficient;
Γ = surface;
Δ = dimension function of D;
δ_{ij} = Kronecker Delta;

ϵ, ϵ^p = volume strain, plastic volume strain;
ε_{ij}, ε_{ij}^p = strain tensor, plastic strain tensor;
η = similarity parameter;
Θ, Θ_s = dimension function of $\theta - \theta_0$ and $\theta_s - \theta_0$;
θ, θ^{ad}, θ_0, θ_s = absolute temperature, adiabatic temperature, initial temperature, surface temperature;
$\bar{\theta}$, $\bar{\theta}_s$ = normalized temperature, normalized surface temperature (similarity parameters);
κ = thermal conductivity;
Λ = dimension function of L;
λ = heat exchange coefficient;
ξ = hydration degree;
ξ_0 = percolation threshold;
ξ = similarity parameter;
σ_{ij} = stress tensor;
τ_h = characteristic hydration time;
Ω = volume;
x' = dimensionless form of variable x;
$\dot{x}$ = time derivative of x;
x° = rate of quantity x;
∇x = gradient of x; and
$\nabla \cdot x$ = divergence of x.